Resetable devices with customised performance for semi-active seismic hazard mitigation of structures

2005 NZSEE Conference

J.G. Chase, K.J. Mulligan, A. Gue, J.B. Mander, T. Alnot & G. Rodgers

Departments of Mechanical and Civil Engineering, University of Canterbury, Christchurch

B. Deam

Leicester Steven EQC Lecturer in Civil Engineering, University of Canterbury, Christchurch

L. Cleeve & D. Heaton

C&M Technologies, Christchurch

ABSTRACT: A one fifth scale semi-active, resetable device is designed and tested. A novel design that utilises each chamber independently allows more flexible control laws than previous resetable devices. Manipulation of the force-displacement hysteresis curve via innovative control laws allows the hysteresis loop to be pre-determined with one such manipulation resulting in removal of energy without increasing the base shear demand. The device characteristics with air as the working fluid, are determined and an analytical model developed. The design stiffness is 250 $kN.m^{-1}$ with the prototype having a stiffness between 185 $kN.m^{-1}$ and 236 $kN.m^{-1}$. The peak force is in excess of 20kN at a displacement of 33mm. The impact of the actuator in a structure is studied using an iterative hybrid approach, a virtual structure, and an experimentally proved device model.

1 INTRODUCTION

Semi-active control is emerging as an effective method of mitigating structural damage from large environmental loads, with two main benefits over active control and passive solutions. First, a large power/energy supply is not required to have a significant impact on response. Second, they provide the broad range of control that a tuned passive system cannot, making them better able to respond to changes in structural behaviour due to non-linearity, damage or degradation over time. Semi-active systems are also strictly dissipative and do not add energy to the system, guaranteeing stability.

Semi-active devices are particularly suitable in situations where the device may not be required to be active for extended periods of time, but may be suddenly required to produce large forces (Bobrow et al., 2000). The potential of semi-active devices and control methods to mitigate damage during seismic events is well documented (e.g. Barroso et al., 2003; Jansen and Dyke, 2000; Yoshida and Dyke, 2004). However, most structural control research, both active and semi-active, has been analytical with very little full scale testing.

Ideally, semi-active devices should be reliable and simple. Resetable devices fit these criteria as they can be constructed with ease and utilise well understood fluids, such as air. These attributes contrast with more complicated semi-active devices such as electro-rheological and magneto-rheological devices to resist motion (Dyke et al, 1996; Spencer et al, 1997). Instead of altering the damping of the system, resetable devices non-linearly alter the stiffness with the stored energy being released as the compressed fluid is allowed to revert to its initial pressure.

Prior to this research the largest capacity test device was approximately 100N and it offered the capability of releasing all the stored energy effectively instantaneously relative to the structural periods being considered (Bobrow and Jabbari, 2002). For larger devices the rate of energy dissipation may be more important as the flow rates required for large systems to release large amounts of stored

energy will potentially be very high. Hence, resetable device design and implementation, while offering significant promise, are still in their infancy.

Semi-active damping via resetable devices also offers the opportunity to sculpt or re-shape the resulting structural hysteresis loop to meet design needs, as enabled by the ability to actively control the device valve and reset times. For example, given a sinusoidal response, a typical viscously damped, linear structure has the hysteresis loop definitions schematically shown in Figure 1a, where the linear force deflection response is added to the circular force-deflection response due to viscous damping to create the well-known overall hysteresis loop. Figure 1b shows the same behaviour for a simple resetable device where all stored energy is released at the peak of each sine-wave cycle and all other motion is resisted (Bobrow and Jabbari, 2002). This form is denoted a "1-4 device" as it provides damping in all four quadrants. A stiff damper will dissipate significant energy, however, the resulting base-shear force is increased. If the control law for the damper is changed such that only motion *towards* the zero position (from the peak values) is resisted, the force-deflection curves that result are shown in Figure 1c. In this case, the semi-active resetable damper force actually reduces the base-shear demand compared to the situation shown in Figures 1a-b. This control law provides significant damping forces only in quadrants 2 and 4, and is denoted a "2-4 device". As a result, the use of controllable semi-active devices offers the opportunity to re-shape and customise the overall structural hysteretic behaviour while also providing supplemental damping to minimise response.

This paper investigates the design, testing and analysis of a one fifth scale resetable device using air as the working fluid. The dynamic and force characteristics of the device are established by experimental tests. The impact and efficacy of different control laws is determined, particularly with respect to the resulting hysteresis loop shape. Once characterised, the ability of the device at reducing the demand on a structure during seismic events is investigated using an experimentally validated model.

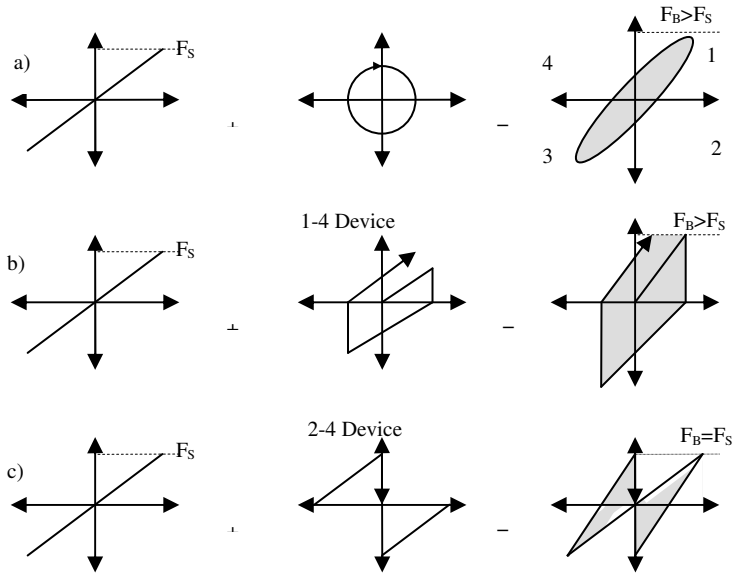

Figure 1: Schematic representation of hysteretic behaviour for a) added or structural viscous damping, b) a resetable device that resists motion between peaks before resetting, and c) a resetable device that resists motion only toward equilibrium and adds damping only in the 2nd and 4th quadrants of the force-deflection plot. The quadrants are labelled in the first panel, and F_B is the total base shear while F_S is the base shear for a linear, undamped structure. $F_B > F_S$ indicates an increase in base shear due to the damping added.

2 DEVICE DYNAMICS

Resetable devices are fundamentally hydraulic spring elements in which the un-stretched spring length can be reset to obtain maximum energy dissipation from the structural system (Bobrow et al. 2000). Energy is stored in the device by compressing the working fluid as the piston is displaced from its

centre position. When the piston reaches its maximum displaced position, the stored energy is also at a maximum. At this point, the stored energy is released by discharging the air to the non-working side of the device, thus resetting the un-stretched spring length. Figure 2 shows the conventional resetable device configuration, with a valve connecting the two sides.

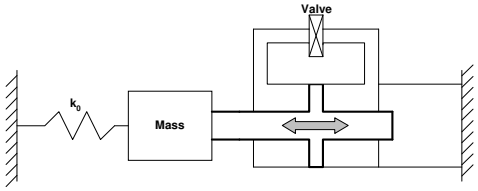

Figure 2: Schematic of semi-active resetable actuator attached to a single degree of freedom system.

Unlike previous resetable devices, the design developed in this research eliminates the need to rapidly dissipate energy using a two-chambered design that utilises each piston side independently, as shown in Figure 3. This approach allows a wider variety of control laws to be imposed as each valve can be operated independently allowing independent control of the pressure on each side of the piston. Air is utilised as the working fluid to make use of the surrounding atmosphere as the fluid reservoir.

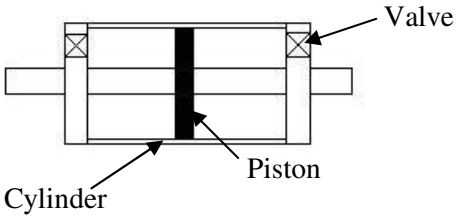

Figure 3: Schematic of independent chamber design. Each valve vents to atmosphere.

Given that air is an ideal gas it obeys the law

$$pV^{\gamma} = c \qquad (1)$$

where γ is the ratio of specific heats, c is a constant and p and V are respectively the pressure and volume in a chamber of the device (Bobrow et al. 2000). Assuming the piston is centred in the device and the initial pressures in both chambers are P_0 with initial volumes V_0 the resisting force is defined:

$$F(x) = (p_2 - p_1)Ac = \left[(V_0 + Ax)^{-\gamma} - (V_0 - Ax)^{-\gamma}\right]Ac \qquad (2)$$

Assuming small motions, Equation (2) can be linearised and an approximate force definition obtained.

$$F(x) = -\frac{2A^2\gamma P_0}{V_0}x \qquad (3)$$

where A is the piston area hence the effective stiffness of the resetable device is defined:

$$k_1 = \frac{2.A^2.\gamma.P_0}{V_0} \qquad (4)$$

3 DESIGN

The device is designed for a one fifth scale, four story steel moment resisting frame with basic dimensions of 2,1x1.2x2.1 meters and a total seismic weight of 35.3kN as described by Kao, (1998). The natural period of the structure is 0.6s, typical of a four-story reinforced concrete building. Given that the total actuator authority has a reasonable value of approximately 15% (Hunt, 2002), and assuming two actuators in the structure a stiffness value of 250 kN.m^{-1} was required. This stiffness results in a force of 2.5kN developed at 10mm displacement of the piston from its centre position.

Trade off curves for a resetable actuator with air as the working fluid show the relationships between parameters. The primary parameters are the diameter, chamber length and maximum piston displacement and are shown in Figure 4. These parameters control the stiffness of the device using Equations (2) to (4). The design space (boxed) is determined by combining these curves with practical, safety and ease of handling constraints. These added constraints include ensuring the length of each chamber is superior to the maximum displacement of the piston, limiting the internal pressure to 2.5 atmospheres, keeping the weight of the device under 20kg and the diameter under 0.2m.

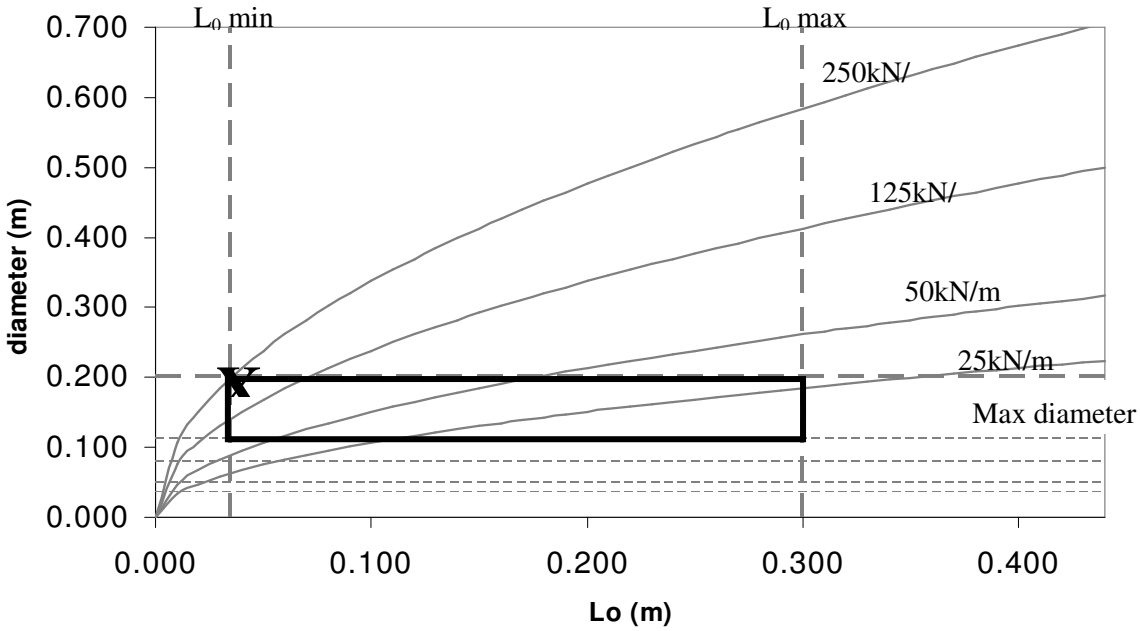

Figure 4: Trade off curve between the diameter and initial chamber length of the device for different stiffness values assuming a maximum piston displacement of 20mm. Each line represents a different stiffness value.

An exploded view of the device is shown in Figure 5a. The piston located inside the cylinder has four seals each located in a groove that ensure minimum air movement between the two chambers. The end caps are press fitted into the cylinder and held in place by four rods. O-rings in the end caps further ensures no leakage of air. Air is prohibited from escaping where the piston rod passes through the end caps by two more seals. An elevation view is shown in Figure 5b.

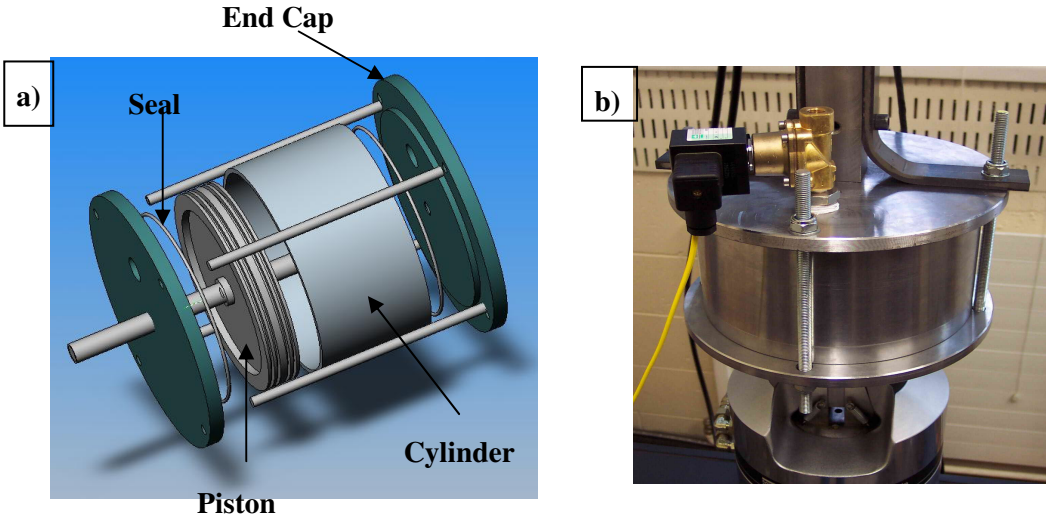

Figure 5: a) Exploded view of prototype indication components, b) Prototype device in MTS test rig.

4 RESULTS

Initial uncontrolled tests with a sine wave piston displacement input indicate the device behaves as expected. The peak force developed at a displacement of 10mm from the centre ranges between 1.85 and 2.36 kN as shown in Figure 7, resulting in a stiffness between 185 $kN.m^{-1}$ and 236 $kN.m^{-1}$ respectively. Reduction in the stiffness from the design value is primarily attributed to air loss via the valves due to valve flexibility. Overall, the force generated is fairly similar for each frequency of input.

Some of the force generated can be attributed to friction between the seals around the piston and the cylinder wall. This contribution is approximately 250N as seen in Figure 8, which shows the force-displacement plot for the device with both valves open and a sine wave input of 10mm at 1Hz and 3Hz. The curved portions of the plot are attributed to Coulomb damping as the air is forced through the open valves which act as an orifice. The faster the air is forced through the restriction the greater the resistance force, as seen in Figure 8 where the 3Hz plot reaches a higher force. Coulomb damping is not observed during controlled tests, however the effect of forcing air through the valve is observed in the significant energy release times required relative to the input motion.

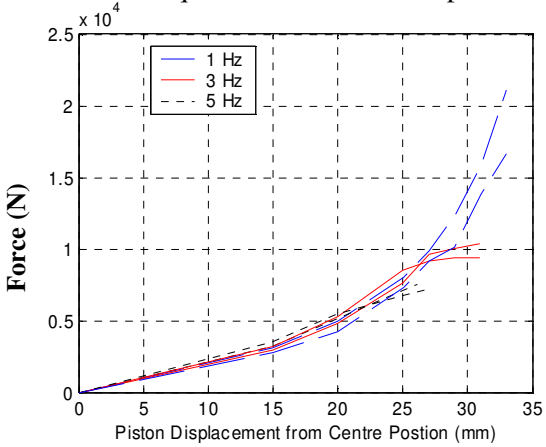

Figure 7: Peak force vs displacement at various input frequencies.

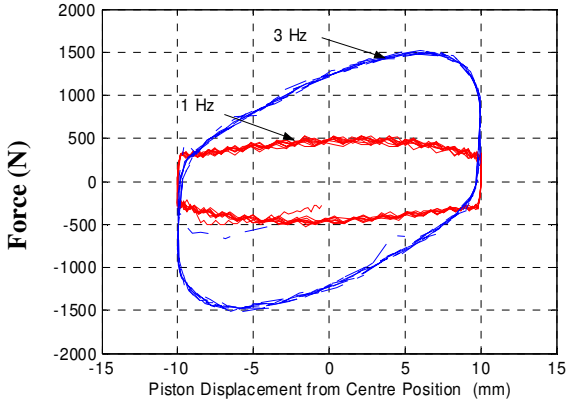

Figure 8: Force vs displacement with both valves open, indicates friction forces between the seals and cylinder.

The 2-4 control law re-shapes the hysteresis loop as it shuts the appropriate valve when the device moves towards the centre position, resisting the return motion of the structure. Figure 9 shows the results for the 2-4 damper, where the model and experimental results are overlaid for a 0.1Hz sinusoidal ground motion of 2 ms^{-2}. Note that offsets or shifts from centre are due to experimental results where the actuator is not exactly centred. In addition, the forces match much better at smaller displacements and forces. Differences in peak forces at larger displacements are due largely to leakage from the valves at higher pressures. Another source of error in this case is due to slightly reduced stiffness delivered by the experimental device in this experiment compared to what is modelled. Finally, note that the hydraulic system running our MTS test system was not able, for unknown

reasons, to provide enough tensile force at higher loads, which may be a partial cause for some error at positive displacements. The forces in quadrants 1 and 3 are due to Coulomb damping when pushing air out of an open orifice as the device returns towards centreline from a sinusoidal peak, per the results in Figure 9. Overall, the model is seen to be a good representation of the physical device.

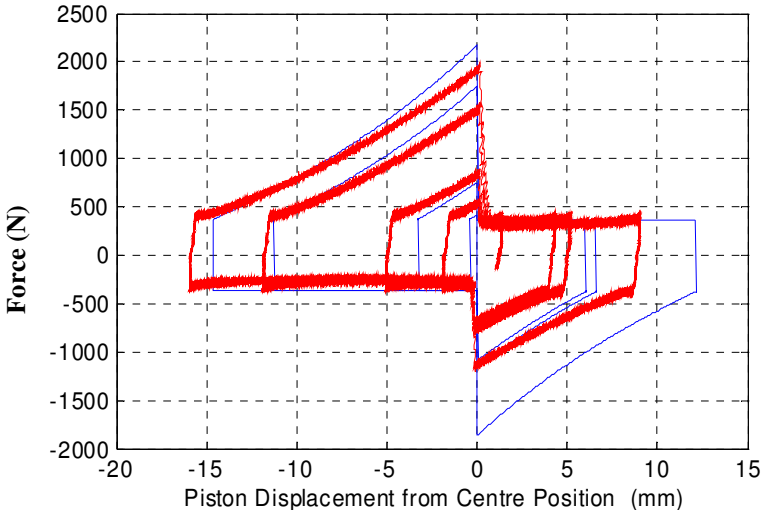

Figure 9: Force vs displacement for a 2-4 device – model versus experimental overlaid.

As expected, the 2-4 device is beneficial in structural control as significant additional energy is removed from the system. Damping in only quadrants 2 and 4 does not increase the base shear, as is evident in both simulation and hybrid test in Figures 10 where 0% structural damping is used for clarity. This last result is potentially important for retrofit applications.

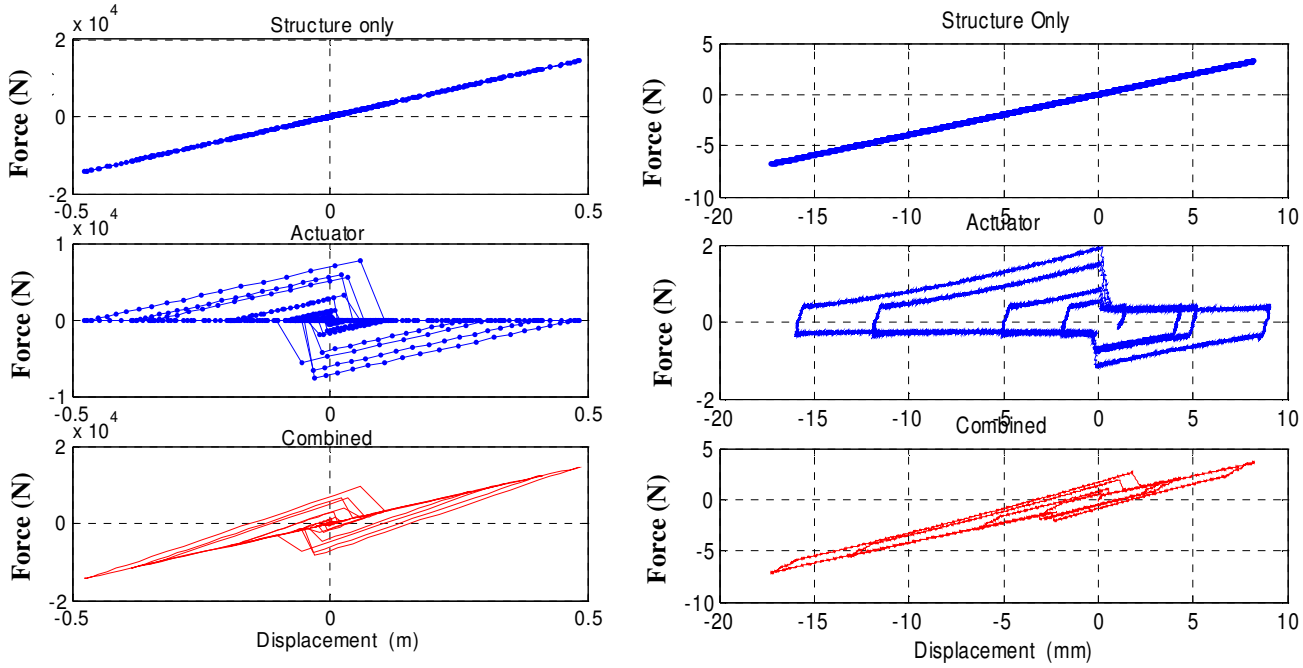

Figure 10: Force-displacement curve for actuator in a single degree of freedom structure with 2-4 control law a) analytical model prediction, b) experimental result. Ground motion is a 2 $m.s^{-2}$ sine wave of frequency 0.1Hz.

To determine the impact for a range of structures, response spectra for the original control law and the 2-4 control are shown in Figures 11. The Kobe record used is scaled for a 2% probability of excedance in 50 years for the Los Angeles area, developed as part of the SAC project (Sommerville et al. 1997). Further investigation is pending in regard to the response spectra for a large suite of ground motion

records. The addition of a resetable device to the structure is beneficial. The reductions in the spectra are substantial when large displacements occur in this near-field event, as large amounts of energy are dissipated when the air is compressed to a higher pressure by larger displacements.

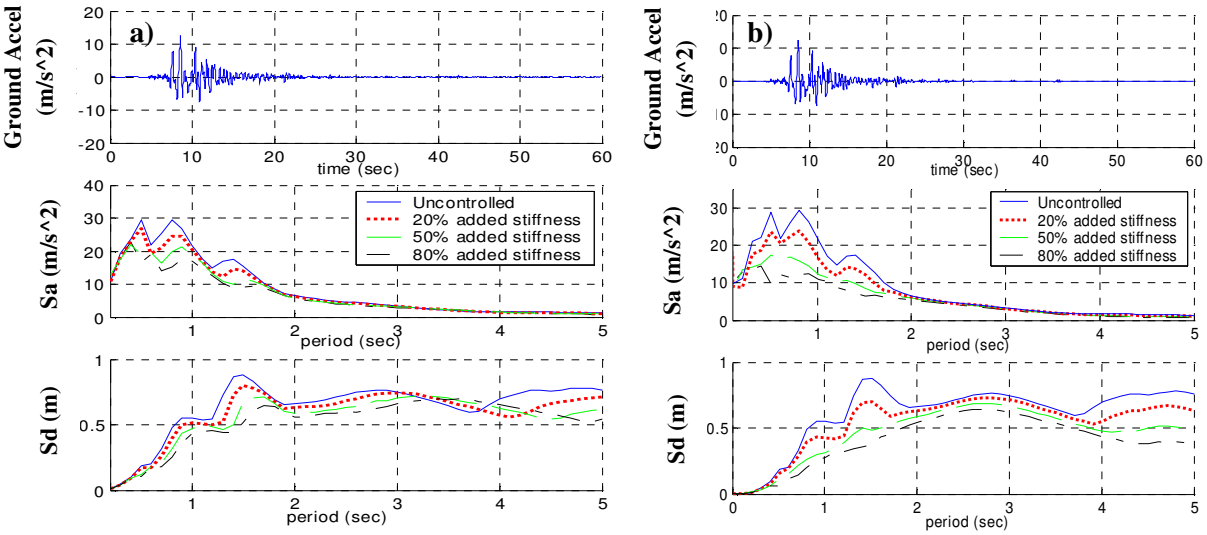

Figure 11: Response spectra for Kobe 1995 (High Suite) with a) Device using original 1-4 control law, b) 2-4 Control law. Structural damping of 5% was used to generate the spectra.

5 CONCLUSIONS

This research has proven that large scale resetable devices, in this case with air as the working fluid, are feasible. It is likely that similar results would be obtained for devices using hydraulic fluids, with the associated increased design complexity. The peak force achieved by the prototype device was in excess of 20kN, which is 200 x times larger than previous, such devices. As a result, the potential design limitations are delineated with further improvements expected in future devices. The resulting stiffness of 185 $kN.m^{-1}$ to 236 $kN.m^{-1}$ was 75-95% of the designed stiffness with most differences associated with less than optimal selection of valves and piston ring seals. Deficiencies in this initial prototype can be readily corrected with more robust design selections for these elements, and better performance would be expected.

A non-linear model of the device in a single degree of freedom system was developed and experimentally validated. An iterative form of hybrid testing was then used to reduce the number and complexity of physical tests required to determine the fundamental performance of different valve control laws. The model also allows different sized devices to be investigated without the need to build numerous prototypes and physically test them. Good correlation between the modelled device and experimental results were found, validating the fundamental models and methods developed.

The novel independent valve design allows more flexible control laws by utilising each chamber independently. This independence results in the ability to manipulate the force-displacement hysteresis curve to obtain an optimal shape for civil structural or other applications. This capability is not available from other proposed resetable device designs that link the two chambers with a single valve. The result of this manipulation is the ability to remove energy from the system without increasing the base shear demand, as seen in the 2-4 device results. Response spectra show a significant improvement can be obtained versus the uncontrolled case, for either the 1-4 or 2-4 control law. More importantly, these spectra show the efficacy of these devices to create more reliable structural energy management in a format (spectra) typically used in structural engineering and design. Finally, the 2-4 control law has the benefit that it does not add to the base shear of the structure, a potential benefit for some retrofit applications.

ACKNOWLEDGEMENTS:

This research was generously supported by the NZ Earthquake Commission Research Foundation (EQC #03/497), for EQC Scholar Ms. Kerry Mulligan.

REFERENCES:

Barroso, L R, Chase, J G and Hunt, S J (2003). "Resetable Smart-Dampers for Multi-Level Seismic Hazard Mitigation of Steel Moment Frames," *Journal of Structural Control*, vol. 10(1), pp. 41-58.

Bobrow, J E, Jabbari, F, Thai, K (2000). "A New Approach to Shock Isolation and Vibration Suppression Using a Resetable Actuator," ASME *Transactions on Dynamic Systems, Measurement and Control,* vol 122, pp. 70-573.

Dyke, S.J, Spencer, B.F, (1996). "Modelling and Control of Magneto-Rheological Dampers for Seismic Response Reduction," *Smart Materials and Structures,* vol 5. pp. 565-575.

Hunt, S, (2002). "Semi-Active Smart-Dampers and Resetable Actuators for Multi-Level Seismic Hazard Mitigation of Steel Moment Resisting Frames," *Masters Thesis, Mechanical Engineering, University of Canterbury, Christchurch.*

Jansen, L M and Dyke, S J (2000). "Semiactive Control Strategies for MR Dampers: Comparative Study," ASCE *J. of Eng. Mechanics*, vol. 126(8), pp. 795-803.

Jabbari, F and Bobrow, J E (2002). "Vibration Suppression with a Resetable Device," ASCE *J. of Eng. Mechanics*, vol. 128(9), pp. 916-924.

Kao, G C, (1998). "Design and Shacking Table Tests of a Four-Storey Miniature Structure Built With Replaceable Plastic Hinges," *Masters Thesis, Civil Engineering, University of Canterbury, Christchurch.*

Sommerville, P, Smith, N, Punyamurthula, S, and Sun, J, (1997). "Development of Ground Motion Time Histories for Phase II of the FEMA/SAC Steel Project." *SAC Background Document Report* No. SAC/BD-97/04.

Spencer, B F, Dyke, S J, Sain, M K, Carlson, J, (1997). "Phenomenological Model for Magneto-Rheological Dampers," ASCE *J. of Eng. Mechanics*, vol 123, pp. 230-238.

Yoshida, O and Dyke, S J, (2004). "Seismic Control of a Nonlinear Benchmark Building Using Smart Dampers," ASCE *J. of Eng. Mechanics*, vol 130(4), pp. 386-392.